



HAL
open science

Optimized Coadministration of Propofol and Remifentanil During the Induction Phase of Total Intravenous Anesthesia With Statistical Validation

Daniel Denardi Huff, Mirko Fiacchini, Thao Dang, Teodoro Alamo

► **To cite this version:**

Daniel Denardi Huff, Mirko Fiacchini, Thao Dang, Teodoro Alamo. Optimized Coadministration of Propofol and Remifentanil During the Induction Phase of Total Intravenous Anesthesia With Statistical Validation. IEEE Control Systems Letters, 2024, 8, pp.193-198. 10.1109/LCSYS.2024.3359529 . hal-04794828

HAL Id: hal-04794828

<https://hal.science/hal-04794828v1>

Submitted on 21 Nov 2024

HAL is a multi-disciplinary open access archive for the deposit and dissemination of scientific research documents, whether they are published or not. The documents may come from teaching and research institutions in France or abroad, or from public or private research centers.

L'archive ouverte pluridisciplinaire **HAL**, est destinée au dépôt et à la diffusion de documents scientifiques de niveau recherche, publiés ou non, émanant des établissements d'enseignement et de recherche français ou étrangers, des laboratoires publics ou privés.

Optimized coadministration of propofol and remifentanil during the induction phase of total intravenous anesthesia with statistical validation

Daniel Denardi Huff, Mirko Fiacchini, Thao Dang and Teodoro Alamo, *Member, IEEE*

Abstract—In this work, a Monte-Carlo approach is proposed to tackle the control design problem of coadministration of propofol and remifentanil during the induction phase of total intravenous anesthesia, where the measured output is the Bispectral Index (BIS). The goal is to minimize the expected value of the Integral Absolute Error of the BIS in presence of high model uncertainties. An additional constraint is used in the resulting optimization problem to limit the probability of a large undershoot of the BIS signal. Simulation results validate the proposed methodology and provide a comparison between the proposed method and another one from the literature.

Index Terms—Total intravenous anesthesia, Monte-Carlo method, Drug control, Optimal control.

I. INTRODUCTION

TOTAL intravenous anesthesia consists in the coadministration of different drugs in order to induce hypnosis (loss of consciousness), analgesia (lack of pain) and areflexia (lack of movement) [1]. In particular, hypnosis and analgesia are mandatory in general anesthesia and are commonly achieved through the use of propofol (a hypnotic drug) and remifentanil (an analgesic drug which also affects the degree of hypnosis). The infusion rates of these drugs must be properly controlled by the anesthesiologist taking into account the particular surgical procedure while avoiding both underdosing, which can lead to partial awakening, and overdosing, which can lead to cardiovascular or respiratory collapse [2] and postoperative complications [3]. In this context, studies have shown the benefits of using automatic closed-loop control for anesthesia, resulting in an improvement of safety for the patient and a reduction of workload for the anesthesiologist [4], [5].

The Bispectral Index (BIS) [6], computed by using the electroencephalographic (EEG) signal, is a well-known and reliable measure of the degree of hypnosis (DoH). This fact, along

This work was partially supported by the LabEx PERSYVAL-Lab under Grant ANR-11-LABX-0025-01. T. Alamo acknowledges support from grant PID2022-142946NA-I00 funded by MCIN/AEI/10.13039/501100011033 and by ERDF, A way of making Europe. Corresponding author: D. D. Huff.

D. D. Huff and M. Fiacchini are with Univ. Grenoble Alpes, CNRS, Grenoble INP, GIPSA-Lab, Grenoble 38000, France (e-mails: {daniel.denardi-huff,mirko.fiacchini}@gipsa-lab.fr).

T. Dang is with Univ. Grenoble Alpes, CNRS, Grenoble INP, VERIMAG, Grenoble 38000, France (e-mail: thao.dang@univ-grenoble-alpes.fr).

T. Alamo is with Department of Systems Engineering and Automation, University of Seville, Seville 41092, Spain (e-mail: talamo@us.es).

with the synergistic effect of propofol and of remifentanil on the DoH, has motivated the use of multiple-input single-output (MISO) control schemes, where the coadministration of these drugs is controlled based only on the BIS signal [7]–[15]. Note that this control structure leads to an additional degree of freedom, since the same steady-state response can be achieved with different input combinations. In [7], for instance, this issue is handled by using empirical rules based on clinical practice, while [8] and [15] propose Model Predictive Control solutions where the balance between the drugs depends on their weights in the corresponding cost functions.

In this work, following the approach of [10]–[14], the ratio between the infusion rates of propofol and remifentanil is fixed. In this way, the anesthesiologist can arbitrarily select the ratio in order to provide the desired hypnotic-opioid balance, which depends on several factors including the specific kind of surgery [16]. However, unlike [10] and [14], the control design problem is solved through a Monte-Carlo approach. The proposed randomized scheme fits into the framework of [17] and has been applied, for instance, in [18] in the case of cancer therapy. The key idea is to take into account the variability of the pharmacokinetic (PK) and pharmacodynamic (PD) parameters of the anesthesia model. That is, the control design is carried out in a stochastic framework where the goal is to minimize the expected value of the chosen performance index under the assumption that the PK and PD parameters follow a log-normal distribution, as reported in [19], [20].

In addition to the stabilization of the BIS output at the desired level during the induction phase of anesthesia, the proposed approach incorporates a constraint to the control design problem whose role is to limit the risk of an excessive undershoot of this signal. In other words, the risk of overdose is reduced, as it will be statistically shown.

The paper is organized as follows. Section II presents the standard PK-PD model for anesthesia. Section III describes the Monte-Carlo approach used to solve the control design problem. Next, Section IV presents the simulation results. At last, some concluding remarks end the paper.

II. STANDARD ANESTHESIA MODEL

Drug administration relies on pharmacokinetic and pharmacodynamic modeling [21]. Pharmacokinetics is the study of drug concentration in different tissues as a function of time and of drug dosing while pharmacodynamics focuses on the relationship between drug concentration and a given physiological

effect. Sections II-A and II-B present, respectively, the PK and PD models considered in this work. The drugs of interest are propofol and remifentanyl and the analyzed physiological effect is the degree of hypnosis, commonly measured through the BIS signal. The latter varies from 0% (no brain activity) to 100% (fully awake patient). It is typically around 50% during general anesthesia, but some variation is acceptable from a clinical perspective, say 40 – 60% [22].

A. Pharmacokinetic model

A three-compartment mammillary PK model is commonly used to describe the distribution of anesthetics in the body, which is divided into three parts: a fast acting compartment (blood) and two additional peripheral compartments (muscle and fat) [19], [20]. Assuming that the drug concentration is approximately homogeneous within each compartment, the resulting model is given by a linear system:

$$\dot{x}(t) = Ax(t) + Bu(t), \quad (1)$$

$$A \triangleq \begin{bmatrix} -\left(\frac{Cl_1}{V_1} + \frac{Cl_2}{V_1} + \frac{Cl_3}{V_1}\right) & \frac{Cl_2}{V_1} & \frac{Cl_3}{V_1} \\ \frac{Cl_2}{V_2} & -\frac{Cl_2}{V_2} & 0 \\ \frac{Cl_3}{V_3} & 0 & -\frac{Cl_3}{V_3} \end{bmatrix}, \quad B \triangleq \begin{bmatrix} 1 \\ \frac{1}{V_1} \\ 0 \end{bmatrix},$$

where the elements of $x(t) \triangleq [x_1(t) \ x_2(t) \ x_3(t)]^T \in \mathbb{R}^3$ represent the drug concentrations in the blood, muscle and fat compartments, respectively, and $u(t)$ is the drug infusion rate. Parameters V_i and Cl_i ($i = 1, 2, 3$) correspond to the volume and clearance rate of the i -th compartment and are functions of the patient's demographic data, that is:

$$\xi = f_\xi(\psi), \quad \text{for all } \xi \in \{V_1, V_2, V_3, Cl_1, Cl_2, Cl_3\}, \quad (2)$$

where $\psi \triangleq (\text{age}, \text{height}, \text{weight}, \text{gender})$. The explicit expressions of the functions $f_\xi : \mathbb{R}^3 \times \{\text{male}, \text{female}\} \rightarrow \mathbb{R}$ in (2) are somewhat cumbersome and can be found in [19] for propofol and in [20] for remifentanyl (see also [23] and [24]). Two different PK models are considered here, one for each drug.

B. Pharmacodynamic model

The PD model describes the impact of the blood concentrations of propofol and of remifentanyl on the BIS signal. It is typically divided into two parts. The first one includes two different first-order linear differential equations (one for each drug) to take into account the delay that exists between a change in the blood concentration $x_1(t)$ and the corresponding change in the effect-site concentration $x_e(t)$:

$$\dot{x}_e(t) = k_e(x_1(t) - x_e(t)). \quad (3)$$

Relation (3) can be represented through the introduction of an effect-site compartment (which corresponds to the brain) in the PK model of Section II-A, as also shown in Fig. 1. The dynamics of $x_1(t)$ in (1) does not need to be modified to take into account the effect-site compartment because the volume of the latter is negligible compared to V_1 .

For propofol we consider [19]:

$$k_e = f_{k_e}(\psi) = 0.146(\text{weight}/70\text{kg})^{-0.25} [\text{min}^{-1}] \quad (4)$$

and for remifentanyl [20]:

$$k_e = f_{k_e}(\psi) = 1.09 \exp(-0.0289(\text{age} - 35\text{yr})) [\text{min}^{-1}]. \quad (5)$$

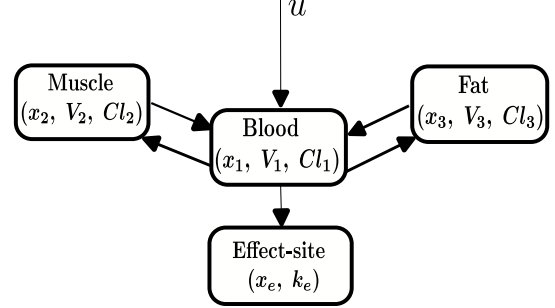


Fig. 1. Pharmacokinetic model.

The second part of the PD model corresponds to a static nonlinear function – a Hill curve – that relates the effect-site concentrations of propofol and remifentanyl, denoted from now on by $x_{e,p}$ and $x_{e,r}$, respectively, to the BIS signal [25]:

$$\text{BIS}(t) = E_0 - E_{\max} \frac{U(t)^\gamma}{1 + U(t)^\gamma}, \quad (6)$$

where $E_0 \approx 100\%$ is a baseline that corresponds to the initial drug-free state of the patient, E_{\max} is the maximal decrease in the BIS signal and γ is a slope coefficient that characterizes the sensibility of the individual to the drugs. The term

$$U(t) \triangleq U_p(t) + U_r(t) \quad (7)$$

describes the combined effect of propofol and remifentanyl on BIS, where

$$U_p(t) \triangleq \frac{x_{e,p}(t)}{C_{50,p}}, \quad U_r(t) \triangleq \frac{x_{e,r}(t)}{C_{50,r}}, \quad (8)$$

and $C_{50,p}$ and $C_{50,r}$ are, respectively, the propofol and remifentanyl half-effect concentrations for BIS [25].

C. Model uncertainties

As previously mentioned, the literature provides equations to compute the parameters of the models for propofol and for remifentanyl as a function of the patient characteristics (i.e. age, height, weight and gender). However, these expressions are just an approximation of the real values, which are subject to uncertainties. The works [19] and [20] propose the use of a log-normal distribution to model the interpatient variability of the PK parameters, which are then treated as random variables. More precisely, (2) is replaced by an expression of the form

$$\xi = f_\xi(\psi) e^{\lambda_\xi}, \quad (9)$$

where $\lambda_\xi \sim \mathcal{N}(0, \sigma_\xi^2)$ is a Gaussian random variable of zero mean and variance σ_ξ^2 for all $\xi \in \{V_1, V_2, V_3, Cl_1, Cl_2, Cl_3\}$. The same reasoning of (9) also applies to parameter k_e in (4) and (5), i.e. $k_e = f_{k_e}(\psi) e^{\lambda_{k_e}}$. Table I presents the variances obtained in [19] for propofol and in [20] for remifentanyl as well as the

nominal values (i.e. with $\lambda_\xi = \lambda_{k_e} = 0$) of the parameters for a 70kg, 170cm, 35-years-old male individual.

	Unit	Propofol		Remifentanil	
		Nominal	σ^2	Nominal	σ^2
V_1	L	6.28	0.610	5.81	0.104
V_2	L	25.50	0.565	8.82	0.115
V_3	L	168.2	0.597	5.03	0.810
Cl_1	L/min	1.62	0.265	2.58	0.0197
Cl_2	L/min	1.83	0.346	1.72	0.0547
Cl_3	L/min	0.77	0.209	0.124	0.285
k_e	1/min	0.146	0.702	1.09	0.947

TABLE I

LOG-NORMAL DISTRIBUTION OF THE PK PARAMETERS. NOMINAL VALUES CORRESPOND TO A 70KG, 170CM, 35-YEARS-OLD MALE INDIVIDUAL.

A log-normal distribution is also proposed in [26] for the PD parameters. The corresponding values are shown in Table II.

	Unit	Nominal	σ^2
$C_{50,p}$	$\mu\text{g/mL}$	4.47	0.0326
$C_{50,r}$	ng/mL	19.3	0.581
γ	–	1.43	0.0884
E_0	%	97.4	0
E_{max}	%	97.4	0

TABLE II

LOG-NORMAL DISTRIBUTION OF THE PD PARAMETERS. NOMINAL VALUES CORRESPOND TO A 70KG, 170CM, 35-YEARS-OLD MALE INDIVIDUAL.

III. CONTROLLER OPTIMIZATION

The control scheme considered in this work (see Fig. 2) is taken from [10], [14] and is based on a parametrized controller denoted by $C(\theta)$, where $\theta \in \mathbb{R}^p$ is the corresponding vector of control parameters. The control inputs are subject to saturation, as also illustrated by Fig. 2. The goal is to regulate the coadministration of propofol and remifentanil during the induction phase of general anesthesia – that is, the patient is initially awake and a setpoint of $r(t) = 50\%$ for the BIS signal must be attained as fast as possible without excessive undershoot. Vector θ will then be tuned based on the minimization of the integral absolute error (IAE), given by

$$IAE \triangleq \int_0^T |r(t) - BIS(t)| dt, \quad (10)$$

where T is the time horizon.

As in [10], [14], a fixed ratio is imposed between the propofol infusion rate, $u_p(t)$ (in mg/s), and the remifentanil infusion rate, $u_r(t)$ (in $\mu\text{g/s}$). In this way, as explained in the introduction, the anesthesiologist can explicitly select the ratio in order to provide the desired hypnotic-opioid balance. In particular, a higher infusion rate of remifentanil implies a stronger analgesic effect. In general,

$$0.5 \leq u_r(t)/u_p(t) \leq 15,$$

where the upper and lower bounds are obtained from clinical considerations described in [10].

A. Tuning of the controller

As explained in Section II-C, the system parameters are uncertain and can be modeled as random variables. Thus, the following optimization problem is proposed to tune the controller $C(\theta)$ such that the expected value of the performance index IAE in (10) is minimized:

$$\theta^* \triangleq \arg \min_{\theta \in \Theta} \mathbb{E}(IAE(\theta, \omega)) \quad (11)$$

where Θ is the search space, $\omega \in \mathbb{R}^{20} \times \{\text{male, female}\}$ represents a concatenation of all the random parameters presented in Table I ($2 \times 7 = 14$ parameters) and in Table II (the first 3 parameters) along with the age, height, weight and gender of the patient and the operator $\mathbb{E}(\cdot)$ denotes expectation with respect to ω . Note that the dependence of IAE on (θ, ω) is made explicit in (11), unlike (10).

In order to cover a wide range of patient profiles, a uniform distribution is considered for the demographic data, where, as in [10], [15]:

$$\begin{aligned} 18\text{yr} &\leq \text{age} \leq 70\text{yr}, \\ 150\text{cm} &\leq \text{height} \leq 190\text{cm}, \\ 50\text{kg} &\leq \text{weight} \leq 100\text{kg}. \end{aligned}$$

Moreover, to reduce the probability of an excessive undershoot of the BIS signal (say $BIS(t) < 40\%$), a constraint of the form

$$\mathbb{E}(g(\alpha, \theta, \omega)) \leq \eta \quad (12)$$

is added to problem (11), where $\eta \in [0, 1]$ and $\alpha \in (0, 100)\%$ are fixed *a priori* and

$$g(\alpha, \theta, \omega) \triangleq \begin{cases} 1, & \text{if } BIS(t) < \alpha \text{ for some } t, \\ 0, & \text{otherwise.} \end{cases} \quad (13)$$

Note from definition (13) that $g(\alpha, \theta, \omega)$ is well-defined (i.e. it is deterministic) for fixed α , θ and ω . Moreover,

$$\mathbb{E}(g(\alpha, \theta, \omega)) = \Pr(BIS(t) < \alpha \text{ for some } t), \quad (14)$$

i.e. $\mathbb{E}(g(\alpha, \theta, \omega))$ corresponds to the probability that the BIS signal goes below the level α during the induction phase of anesthesia when the control parameters are given by θ and taking into account the probability distribution of ω . Constraint (12) imposes an upper bound for this probability.

It is not an easy task to compute the exact value of the expectations in (11) and (12), as remarked in [17]. Thus, as proposed in this reference, a Monte-Carlo approach is used to tackle the control design problem. The key idea is to draw a cloud

$$\Omega \triangleq \{\omega^{(j)}\}_{j=1}^N$$

of N independent realizations of the random vector ω according to its known probability distribution. Then, the optimization problem composed by (11) and (12) can be approximately solved by considering the sample means of $IAE(\theta, \omega)$ and $g(\alpha, \theta, \omega)$, i.e.

$$\hat{\theta} = \arg \min_{\theta \in \Theta} \hat{\mathbb{E}}_{IAE}(\theta, \Omega) \quad (15)$$

$$\text{such that } \hat{\mathbb{E}}_g(\alpha, \theta, \Omega) \leq \eta,$$

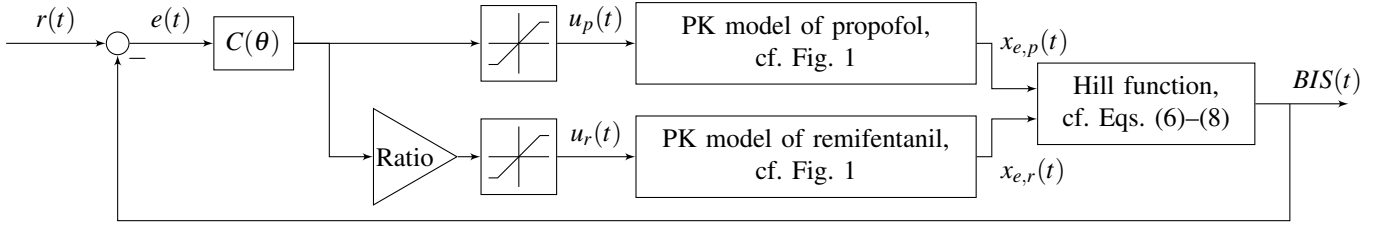


Fig. 2. Control scheme for coadministration of propofol and remifentanyl during general anesthesia. Adapted from [10].

where

$$\hat{\mathbb{E}}_{IAE}(\theta, \Omega) \triangleq \frac{1}{N} \sum_{j=1}^N IAE(\theta, \omega^{(j)}),$$

$$\hat{\mathbb{E}}_g(\alpha, \theta, \Omega) \triangleq \frac{1}{N} \sum_{j=1}^N g(\alpha, \theta, \omega^{(j)}).$$

Note that, with this procedure, the original constraint (12) is *not* necessarily satisfied for $\theta = \hat{\theta}$ obtained in (15). However, it is possible to obtain a confidence interval (CI) for the value of $\mathbb{E}(g(\alpha, \hat{\theta}, \omega))$ *a posteriori*, as it will be shown next. Moreover, if desirable, one can replace η in (15) by a smaller value $\eta' < \eta$ in order to reduce the chances of violation of (12) (see [27]).

B. Statistical analysis

Even if the probability of a large undershoot as in (14) is not known, it is possible to infer its value from the sample mean $\hat{\mathbb{E}}_g(\alpha, \theta, \Omega)$ with a certain confidence level $(1 - \delta)$, where $\delta \in (0, 1)$. In order to do so, consider a cloud Ω' of N' new realizations of ω (independent of the realizations used to design the controller). Given $\hat{\theta}$ from (15), δ and N' , a $100(1 - \delta)\%$ confidence interval for $\mathbb{E}(g(\alpha, \hat{\theta}, \omega))$ can be computed as in [28]:

$$\hat{p} \pm z_{\delta/2} \sqrt{\hat{p}(1 - \hat{p})/N'} \quad (16)$$

where $\hat{p} \triangleq \hat{\mathbb{E}}_g(\alpha, \hat{\theta}, \Omega')$ and z_c denotes the $(1 - c)$ quantile of the standard normal distribution¹. This is known as the Wald confidence interval. Note that a larger value of N' results in a smaller interval for the same confidence level.

IV. SIMULATION RESULTS

To illustrate the proposed approach, consider, as in [10], [14], that $C(\theta)$ corresponds to a standard PID controller:

$$C(\theta) \triangleq K_p \left(1 + \frac{1}{T_i s} + \frac{T_d s}{1 + T_d s/M} \right), \quad (17)$$

where K_p is the proportional gain, T_i is the integral time constant, T_d is the derivative time constant and the high-frequency pole of the derivative term depends on the factor $M = 5$. In practice, the BIS signal is very noisy and, thus, care should be taken to avoid a high value of T_d , which could be detrimental.

¹A typical value is $z_{\delta/2} = 1.96$ for $\delta = 0.05$, i.e. 95% of confidence.

The control loop is implemented in a sampled-data fashion using a sampling period of 1 second as in [10], [15]. Thus, in practice, (17) is discretized and (10) is replaced by a summation over a finite time horizon of 10min. Moreover, considering the maximum infusion rate of a standard clinical pump, one concludes that $0 \leq u_p(t) \leq 6.67 \text{ mg/s}$ and that $0 \leq u_r(t) \leq 16.67 \mu\text{g/s}$ [10]. Taking these limits into account, a conditional integration anti-windup technique from [29] has been implemented in the controller block of Fig. 2.

Problem (15) is solved with $\alpha = 40\%$ for different values of the parameter η through the particle swarm optimization algorithm (PSO) [30] with a swarm size of 100 particles. The simulation results consider $u_r(t)/u_p(t) = 2$, which is a typical value for the ratio of drugs in normal conditions [10]. The number of Monte-Carlo samples is fixed at $N = 1000$, $\theta \triangleq [K_p \ T_i \ T_d]^T \in \mathbb{R}^3$ and the search space Θ is an empirically chosen hypercube:

$$\Theta \triangleq [1.6 \times 10^{-3}, 3.2 \times 10^{-1}] \times [10^2, 10^3] \times [10^{-1}, 10^2] \subset \mathbb{R}^3.$$

The closed-loop system is simulated through the Python Anesthesia Simulator presented in [31], which includes different well-known models for anesthesia, among them the ones mentioned in Section II.

PID	η	K_p	T_i	T_d	$\hat{\mathbb{E}}_{IAE}(\hat{\theta}, \Omega)$	$\hat{\mathbb{E}}_g(\alpha, \hat{\theta}, \Omega)$
#1	—	0.0549	588.3	10.25	3539	18.1%
#2	10%	0.0443	624.2	12.17	3650	10%
#3	5%	0.0398	738.4	14.24	3854	5%
#4	2%	0.0289	655.1	21.88	4595	2%
#5	1%	0.0244	731.0	21.51	5152	0.9%
#6	0.5%	0.0197	599.6	31.49	5963	0.5%
#7 [10]	—	0.0924	916.3	19.75	—	—

TABLE III

COMPUTED PID CONTROLLERS AND CORRESPONDING VALUES OF THE SAMPLE MEANS $\hat{\mathbb{E}}_{IAE}(\hat{\theta}, \Omega)$ AND $\hat{\mathbb{E}}_g(\alpha, \hat{\theta}, \Omega)$ OBTAINED THROUGH THE SOLUTION OF (15).

Table III shows the PID controllers obtained through the solution of (15) as well as the resulting sample means $\hat{\mathbb{E}}_{IAE}(\hat{\theta}, \Omega)$ and $\hat{\mathbb{E}}_g(\alpha, \hat{\theta}, \Omega)$. The *a posteriori* statistical analysis of these controllers will be presented in Section IV-A. Controller #1 was obtained without the use of constraint $\hat{\mathbb{E}}_g(\alpha, \theta, \Omega) \leq \eta$. For comparison purposes, the table also shows the PID controller obtained with the method from [10], which is tuned by solving a min-max optimization problem of the form:

$$\hat{\theta} = \underset{\theta \in \Theta}{\operatorname{argmin}} \max_{\psi \in \Psi} IAE(\theta, \psi) \quad (18)$$

where $\psi = (\text{age, height, weight, gender}) \in \Psi$ varies within a predefined list of 13 patients (cf. Table 1 in [10]), which is

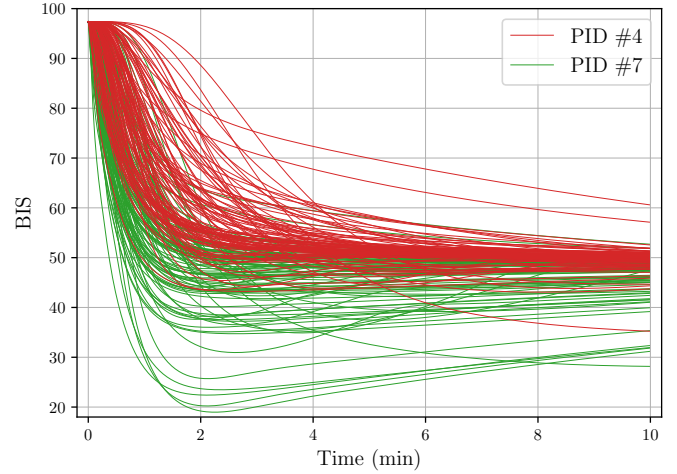
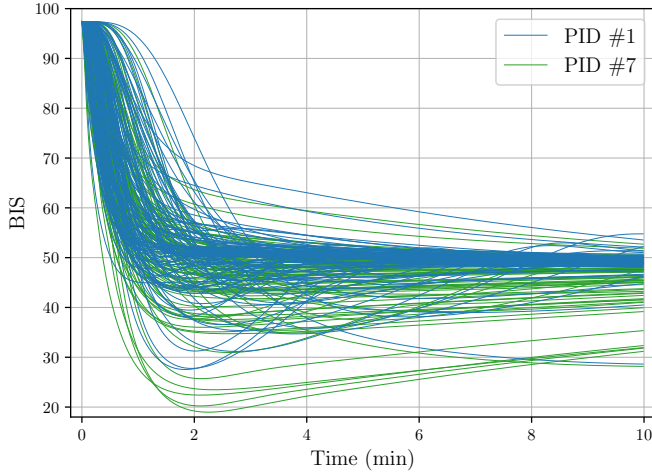


Fig. 3. BIS output of the closed-loop system for 100 patients randomly chosen from cloud Ω' .

representative of a wide population with significantly different responses to propofol and remifentanyl administration, as argued in the aforementioned reference. In this case, the inpatient variability of the PK-PD parameters is not taken into account in the computation of IAE in (18), i.e. the model uncertainties described in Section II-C are not directly used.

As shown by Table III, the use of a more restrictive parameter η in constraint (12) results in a larger value of IAE. In other words, there exists a compromise between the performance index IAE and the probability of a large undershoot of the BIS signal. This fact is confirmed in the next section, where a numerical analysis of the obtained PID controllers is performed.

A. Numerical analysis

The procedure of Section III-B is used to analyze the controllers presented in Table III. The number of samples for the Monte-Carlo runs is fixed at $N' = 10N = 10000$. The resulting sample means $\hat{\mathbb{E}}_{IAE}(\hat{\theta}, \Omega')$ are shown in Table IV, as well as the 99% confidence intervals for $\mathbb{E}(g(\alpha, \hat{\theta}, \omega))$.

PID	$\hat{\mathbb{E}}_{IAE}(\hat{\theta}, \Omega')$	99% CI for $\mathbb{E}(g(\alpha, \hat{\theta}, \omega))$
#1	3583	[15.91%, 17.83%]
#2	3727	[9.68%, 11.26%]
#3	3926	[5.97%, 7.25%]
#4	4665	[2.06%, 2.86%]
#5	5214	[1.03%, 1.63%]
#6	6025	[0.74%, 1.26%]
#7 [10]	4569	[22.42%, 24.6%]

TABLE IV

STATISTICAL ANALYSIS OF THE PID CONTROLLERS OF TABLE III.

Recall that $\mathbb{E}(g(\alpha, \hat{\theta}, \omega))$ is the probability of a large undershoot of the BIS signal during the induction phase of anesthesia – in this case, the probability that the BIS goes below the level $\alpha = 40\%$. As indicated by Table IV, the reduction of this probability results in a less aggressive control law in the sense that the expected value of the performance index IAE – approximately given by $\hat{\mathbb{E}}_{IAE}(\hat{\theta}, \Omega')$ – increases. Thus, there exists a compromise between these

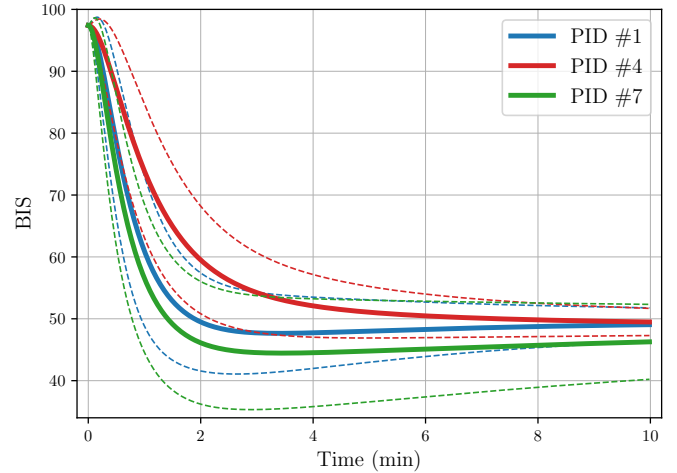


Fig. 4. Mean value of the BIS \pm its standard deviation over the cloud Ω' of $N' = 10000$ patients for the PIDs.

two performance criteria that must be taken into account by the anesthesiologist in order to choose the most appropriate controller between the options of Table IV.

As also shown by Table IV, the expected value of IAE for the PIDs #1, #2 and #3 is smaller than the one for PID #7, obtained with the approach from [10]. Moreover, all controllers from #1 to #6 result in smaller probabilities of large undershoot than PID #7 according to the 99% confidence intervals for $\mathbb{E}(g(\alpha, \hat{\theta}, \omega))$. In particular, PID #4 provides a probability of large undershoot around 10 times smaller than the one of PID #7 while the expected value of IAE for these two controllers is roughly the same.

The facts described above are corroborated by Figs. 3 and 4, which provide a more detailed comparison between PIDs #1, #4 and #7. Fig. 3 shows the resulting BIS output of the closed-loop system for 100 patients randomly chosen from cloud Ω' while Fig. 4 presents the mean value of the BIS \pm its standard deviation over Ω' . Note in Fig. 3 that the designed controllers may result in a significant undershoot of the BIS for some realizations of the system. This is expected from the

fact that $\mathbb{E}(g(\alpha, \hat{\theta}, \omega))$, even if small, is not exactly equal to zero.

V. CONCLUSIONS

A Monte-Carlo approach was presented to tackle the control design problem of coadministration of propofol and remifentanil during the induction phase of total intravenous anesthesia, where the goal is to minimize the expected value of the IAE of the BIS and, at the same time, limit the probability of a large undershoot of this signal. As shown by the simulations, there is a compromise between these two criteria. Moreover, compared to the controller from [10], the ones provided by the proposed method result in considerably smaller probabilities of a large undershoot of the BIS while the expected value of the IAE is of the same order of magnitude.

The framework is quite flexible and can handle other performance criteria – like the settling time or time to target – as well as other types of control law, which could be investigated in the future. Another possibility of future work is to combine the idea of individualized PID tuning considered in [14] with the Monte-Carlo approach presented in this paper in order to improve the performance of the resulting closed-loop system. Moreover, the maintenance phase of anesthesia could also be studied. Finally, it would also be possible to consider measurement noise within the proposed framework, taking into account that the BIS signal is usually considerably noisy.

REFERENCES

- [1] D. Copot, *Automated drug delivery in anesthesia*. Academic Press, 2020.
- [2] S. Bibian, C. R. Ries, M. Huzmezan, and G. Dumont, "Introduction to automated drug delivery in clinical anesthesia," *European Journal of Control*, vol. 11, no. 6, pp. 535–557, 2005.
- [3] M. T. Chan, B. C. Cheng, T. M. Lee, and T. Gin, "BIS-guided anesthesia decreases postoperative delirium and cognitive decline," *Journal of Neurosurgical Anesthesiology*, vol. 25, no. 1, pp. 33–42, 2013.
- [4] N. Liu, T. Chazot, A. Genty, A. Landais, A. Restoux, K. McGee, P.-A. Laloë, B. Trillat, L. Barvais, and M. Fischler, "Titration of propofol for anesthetic induction and maintenance guided by the bispectral index: Closed-loop versus manual control: A prospective, randomized, multicenter study," *Anesthesiology*, vol. 104, no. 4, pp. 686–695, 2006.
- [5] L. M. Pasin, P. M. Nardelli, M. M. Pintaudi, M. M. Greco, M. M. Zambon, L. M. Cabrini, and A. M. Zangrillo, "Closed-loop delivery systems versus manually controlled administration of total IV anesthesia: A meta-analysis of randomized clinical trials," *Anesthesia & Analgesia*, vol. 124, no. 2, pp. 456–464, 2017.
- [6] I. Rampil, "A primer for EEG signal processing in anesthesia," *Anesthesiology*, vol. 89, no. 4, pp. 980–1002, 1998.
- [7] N. Liu, T. Chazot, S. Hamada, A. Landais, N. Boichut, C. Dussaussoy, B. Trillat, L. Beydon, E. Samain, D. I. Sessler *et al.*, "Closed-loop coadministration of propofol and remifentanil guided by bispectral index: a randomized multicenter study," *Anesthesia & Analgesia*, vol. 112, no. 3, pp. 546–557, 2011.
- [8] C. M. Ionescu, R. De Keyser, and M. M. Struys, "Evaluation of a propofol and remifentanil interaction model for predictive control of anesthesia induction," in *2011 50th IEEE Conference on Decision and Control and European Control Conference*, 2011, pp. 7374–7379.
- [9] K. Soltesz, G. A. Dumont, K. van Heusden, T. Hägglund, and J. M. Ansermino, "Simulated mid-ranging control of propofol and remifentanil using EEG-measured hypnotic depth of anesthesia," in *51st IEEE Conference on Decision and Control*, 2012, pp. 356–361.
- [10] L. Merigo, F. Padula, N. Latronico, M. Paltenghi, and A. Visioli, "Optimized PID control of propofol and remifentanil coadministration for general anesthesia," *Communications in Nonlinear Science and Numerical Simulation*, vol. 72, pp. 194–212, 2019.
- [11] —, "Event-based control tuning of propofol and remifentanil coadministration for general anaesthesia," *IET Control Theory & Applications*, vol. 14, no. 19, pp. 2995–3008, 2020.
- [12] M. Schiavo, F. Padula, N. Latronico, L. Merigo, M. Paltenghi, and A. Visioli, "Performance evaluation of an optimized PID controller for propofol and remifentanil coadministration in general anesthesia," *IFAC Journal of Systems and Control*, vol. 15, p. 100121, 2021.
- [13] M. Schiavo, F. Padula, N. Latronico, M. Paltenghi, and A. Visioli, "A modified PID-based control scheme for depth-of-hypnosis control: Design and experimental results," *Computer Methods and Programs in Biomedicine*, vol. 219, p. 106763, 2022.
- [14] —, "Individualized PID tuning for maintenance of general anesthesia with propofol and remifentanil coadministration," *Journal of Process Control*, vol. 109, pp. 74–82, 2022.
- [15] B. Aubouin-Pairault, M. Fiacchini, and T. Dang, "Automated multi-drugs administration during total intravenous anesthesia using multi-model predictive control," *arXiv:2309.08229*, 2023.
- [16] J. Vuyk, M. Mertens, E. Olofsen, A. L. Burm, and J. Bovill, "Propofol anesthesia and rational opioid selection : Determination of optimal EC50-EC95 propofol-opioid concentrations that assure adequate anesthesia and a rapid return of consciousness," *Anesthesiology*, vol. 87, no. 6, pp. 1549–1562, 1997.
- [17] T. Alamo, R. Tempo, A. Luque, and D. R. Ramirez, "Randomized methods for design of uncertain systems: Sample complexity and sequential algorithms," *Automatica*, vol. 52, pp. 160–172, 2015.
- [18] M. Alamir, "Learning-based sensitivity analysis and feedback design for drug delivery of mixed therapy of cancer in the presence of high model uncertainties," *Journal of Theoretical Biology*, vol. 568, p. 111508, 2023.
- [19] D. Eleveld, P. Colin, A. Absalom, and M. Struys, "Pharmacokinetic–pharmacodynamic model for propofol for broad application in anaesthesia and sedation," *British Journal of Anaesthesia*, vol. 120, no. 5, pp. 942–959, 2018.
- [20] D. J. Eleveld, J. H. Proost, H. Vereecke, A. R. Absalom, E. Olofsen, J. Vuyk, and M. M. R. F. Struys, "An allometric model of remifentanil pharmacokinetics and pharmacodynamics," *Anesthesiology*, vol. 126, no. 6, pp. 1005–1018, 2017.
- [21] J. Bailey and W. Haddad, "Drug dosing control in clinical pharmacology," *IEEE Control Systems Magazine*, vol. 25, no. 2, pp. 35–51, 2005.
- [22] C. Rosow and P. J. Manberg, "Bispectral index monitoring," *Anesthesiology Clinics of North America*, vol. 19, no. 4, pp. 947–966, 2001.
- [23] T. Schnider, C. Minto, P. Gambus, C. Andresen, D. Goodale, S. Shafer, and E. Youngs, "The influence of method of administration and covariates on the pharmacokinetics of propofol in adult volunteers," *Anesthesiology*, vol. 88, no. 5, pp. 1170–1182, 1998.
- [24] C. Minto, T. Schnider, T. Egan, E. Youngs, H. M. Lemmens, P. Gambus, V. Billard, J. Hoke, K. P. Moore, D. Hermann, K. Muir, J. Mandema, and S. Shafer, "Influence of age and gender on the pharmacokinetics and pharmacodynamics of remifentanil: I. model development," *Anesthesiology*, vol. 86, no. 1, pp. 10–23, 1997.
- [25] C. Minto, T. Schnider, T. Short, K. Gregg, A. Gentilini, and S. Shafer, "Response surface model for anesthetic drug interactions," *Anesthesiology*, vol. 92, no. 6, pp. 1603–1616, 2000.
- [26] T. Bouillon, J. Bruhn, L. Radulescu, C. Andresen, T. Shafer, C. Cohane, and S. Shafer, "Pharmacodynamic interaction between propofol and remifentanil regarding hypnosis, tolerance of laryngoscopy, bispectral index, and electroencephalographic approximate entropy," *Anesthesiology*, vol. 100, no. 6, pp. 1353–1372, 06 2004.
- [27] T. Alamo, R. Tempo, and A. Luque, "On the sample complexity of randomized approaches to the analysis and design under uncertainty," in *American Control Conference*, 2010, pp. 4671–4676.
- [28] A. Agresti and B. A. Coull, "Approximate is better than "exact" for interval estimation of binomial proportions," *The American Statistician*, vol. 52, no. 2, pp. 119–126, 1998.
- [29] A. Visioli, *Practical PID control*. Springer Science & Business Media, 2006.
- [30] J. Kennedy and R. Eberhart, "Particle swarm optimization," in *International Conference on Neural Networks*, vol. 4, 1995, pp. 1942–1948.
- [31] B. Aubouin-Pairault, M. Fiacchini, and T. Dang, "PAS: a Python Anesthesia Simulator for drug control," *Journal of Open Source Software*, vol. 8, no. 88, p. 5480, 2023.